AIAA JOURNAL
Vol. 38, No. 12, December 2000

Nonelectrical Tube Explosive Transfer System

Lien C. Yang* and Ian H. P. Do†
TRW Systems and Information Technology Group, San Bernardino, California 92408

Analyses of internal ballistics and criteria for reaction propagation in nonelectrical tube explosive lines were performed based on explosive loading density, average particle size, and typical geometry using an approach based on heat transfer and decomposition kinetics in the explosive particles in quasi steady state. The results indicate the existence of a critical or maximum average explosive particle size for a given explosive loading density beyond which sustained propagation may cease. Large variations usually exist in the explosive loading density, so that fine particle sizes below 20 θ m are preferable. Fine particle size also may increase the adhesion to the inner tube wall for mitigation of powder migration problems. Computer simulations of detonating end tip to nondetonating end tip transfer were performed using the CTH hydrodynamic code developed by the Sandia National Laboratories. Preliminary results indicate that the hot gas from the detonating end tip is more effective for initiating pyrotechnics in the nondetonating end tip and that a larger gap between the end tips is essential for the success of hot gas initiation.

Nomenclature

A	=	preexponential factor, s^{-1}
a	=	initial radius of HMX particle, μm
a_c	=	critical average HMX particle radius, μm
B	=	activation energy, K
C_p	=	specific heat, cal/g-°C
D_c	=	critical average HMX particle diameter, μm
$(dE/dt)_1$	=	rate of energy loss per unit length in the reaction zone in the nonelectrical (NONEL) tube, cal/m-s
$(dE/dt)_2$	=	rate of energy per unit length created by HMX decomposition in the reaction zone in the NONEL tube, cal/m-s
E	=	energy per unit length in the reaction zone, cal/m
e_0	=	specific heat of explosion, cal/g
e_1	=	specific energy, cal/g
K	=	thermal conductivity, cal/s-cm-°C
ℓ	=	average HMX layer thickness, μm
N	=	number of HMX particles with uniform radius a per unit length, m^{-1}
P	=	peak pressure in NONEL tube, MPa
P_i	=	impact pressure, GPa
p_1	=	vapor pressure of liquid HMX, mm Hg
p_2	=	vapor pressure of solid HMX, mm Hg
r	=	radius of interior of HMX particles that have not decomposed, μm
$\dot{r}_0$	=	rate of HMX regression, μm/μs
T	=	temperature [Eqs. (1–3)], °C or K
T_i	=	impact temperature, K
$T_{surface}$	=	surface temperature of HMX particles, °C
T_0	=	background temperature, °C
t	=	time of heating, s
V_i	=	impact velocity, km/s
v_0	=	volume per unit length in the NONEL tube, cm^3/m
w	=	weight of HMX at given t
w_0	=	initial weight of HMX
x	=	normalized value of r, equal to r/a
Δt	=	heating time of HMX at a given T for $\Delta w/w_0$ equals 0.99
$\Delta w/w_0$	=	fractional weight loss of HMX
κ	=	thermal diffusivity, cm^2/s
λ	=	linear explosive loading density, mg/m
λ_0	=	critical linear explosive loading density, 5 mg/m
ρ	=	density, g-cm^{-3}
τ	=	normalized time, $\kappa t/a^2$
τ_1	=	thermal time constant of 1-mm i.d. HALAR tube, μs

Introduction

A TYPICAL nonelectrical (NONEL) tube explosive transfer system (ETS) consists of a plastic tube of approximately 1 mm i.d. and 3 mm o.d. with a thin layer of explosive material coating deposited on its inner wall during the tube extrusion process (Fig. 1). When properly initiated, a shock wave is established in the tube and propagates at a supersonic speed of from ~1.4 to ~1.9 km/s (~4600 to ~6200 ft/s). The NONEL tube was invented in the late 1960s by Nitro Nobel AB in Sweden.[1] Subsequently, it was licensed in the United States by several explosive companies under different trade names, for example, Primadet nonelectric delay detonators, shock tube assembly (STA), and thin-layer explosive (TLX).

The NONEL tube is an ingenious device because it has a high propagation speed and a minute amount of explosives, usually on the order of 10^{-2} g/m. This makes it a very safe and lightweight device. Demonstrations have shown that it is survivable in many adverse environments. For a better handling resistance, steel overbraids were added on the exterior of the line in TLX. Since the 1970s, it has gradually been adopted in a variety of ordnance systems in which ETS is required, for example, blasting in mining, quarrying, and construction[2]; crew escape systems in military aircrafts; ordnance systems in launch vehicles and missiles; and launch vehicle flight termination systems, which require the highest functional reliability. To date, several hundred thousand devices have been manufactured and used in the United States. It is considered a well-established technology.

Several TLX failures, however, were encountered recently in one major launch vehicle program (Delta III). These failures impacted all flight termination systems using this design, including the Multi-Service Launch Program and Taurus Vehicle Program. There were propagation failures in the lines and failures in the detonating [high-energy explosive (HE)] end-tip-to-deflagrating [low-energy explosive (LE)] end-tip transfer.[3] Much of the design information that affects performance of the device is proprietary to the manufacturers. This limitation impedes the understanding of the device, which limits opportunities to avoid failure modes and to improve process controls to prevent failures. Also, there are no analyses or technical papers in the public domain regarding how this device works and the effects of various design parameters. It is the intent of this paper to present analyses using nonproprietary information, that is, in the

Presented as paper 99-2420 at the AIAA/ASME/SAE/ASEE 35th Joint Propulsion Conference, Los Angeles, CA, 20–24 June 1999; received 30 September 1999; revision received 3 March 2000; accepted for publication 12 May 2000.

*Senior Staff Engineer, Propulsion, Structures and Fluid Mechanics Technical Center, Space and Missile Systems Division, 1475 E. Harry Sheppard Boulevard. Member AIAA.

†Member Technical Staff, Structures and Fluid Mechanics Technical Center, Space and Missile Systems Division, 1475 E. Harry Sheppard Boulevard.

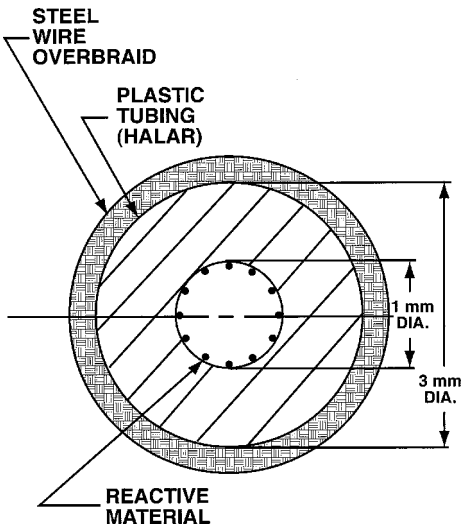

Fig. 1 NONEL tube concept.

public domain, to advance understanding of NONEL tube operation, and based on the results, to recommend possible processing control and reliability improvements.

Information in Public Domain

The information available in the public domain is as follows:

1) Nitro Nobel AB's U.S. patent[1] on the NONEL tube;

2) Ensign Bickford Company, Simsbury, Connecticut, sales catalog for Primadet products family;

3) OEA Aerospace, Inc., Fairfield, California, sales brochure for TLX; and

4) TLX application on military aircraft papers.[4,5]

A variety of explosives can be used for the NONEL tube: PETN, RDX, HMX, tetryl, TNT, etc. (for formal and alternative names see Refs. 6 and 7). The tube can have different inner diameters and be initiated by a detonator or spark, and the tube output can initiate primer or delay pyrotechnic based detonating explosive train. Items 3 and 4 from preceding list provide the following information: tube dimension, 1 mm i.d. and 3 mm o.d.; propagation speed, 1.4–1.75 km/s (4600–5700 ft/s); peak pressure, 27.58 MPa (4000 psi); pressure pulse duration, ~25 μs; HE end-tip composition, lead-azide/HNS-I (see Refs. 6 and 7); LE end-tip composition, ignition strand, a pyrotechnic composition; tube material, HALAR, trade name of an extrudable fluorapolymer manaufactured by Ausimont USA, Inc., Thorofare, New Jersey; tube explosives, mixture of aluminum and HMX; explosive loading density, 20 ± 10 mg/m; braids material, corrosive resistant steel; propagation length in absence of explosive coating and under ideal conditions of straight length geometry, all-fire gap of 19.1 cm (7.5 in.), 50%-fire gap of 29.2 cm (11.5 in.), and no-fire gap of 47.7 cm (18.0 in.).

In addition, Ref. 3 provides the following information regarding Delta III TLX failures:

1) Leak testing of sealed but leaking TLX caused the explosive powder on the inner wall of TLX to be scrubbed off and to leave portions of the cord bare; therefore, explosive propagation failed in the bare portion of the tube. Corrective action is do not rework a leaking TLX; throw the line away.

2) HE end-tip shrapnel damaged LE end tip; therefore, the latter failed to initiate. Corrective action is to add an adapter between the two end tips to filter out the shrapnel.

A preliminary survey was conducted to determine what analytical approaches exist and what approach might be useful to generate an analytical model. There is no previous work that can be directly applied to model NONEL tube operation. Close resemblance exists in the coal dust explosion and silo grain dust explosion. However, in these cases, the reactions depend on oxygen content in the air, that is, oxygen diffusion is a limiting factor. The attainable pressures in these types of phenomena are considerably lower than that in a NONEL tube. Conversely, to treat the problem as a two-phase detonation propagation appears unrealistic because the pressure in a NONEL tube is low as compared to that observed in the detonation of a high explosive.

Table 1 Extrapolated p_1, $\Delta w/w_0$, and Δt as a function of T

T, °C	p_1, mm Hg (psi)	$\Delta w/w_0$	Δt
275	0.30	1.26×10^{-6}	91.1 s
350	4.72	4.25×10^{-4}	0.27 s
400	21.0	9.96×10^{-3}	0.012 s
450	79.3	0.141	7.57×10^{-4} s
500	233.1	0.800	7.07×10^{-5} s
609.7	1,753	1.00	1 μs
683.1	5,181	N/A	0.1 μs (?)
800	21,590 (418)	N/A	4 ns (?)
950	92,327 (1,747)	N/A	N/A
1,000	135,038 (2,312)	N/A	N/A
1,050	195,838 (3,788)	N/A	N/A

There will be a serious shortcoming in treating the problem as a gas-phase shock wave propagation enhanced by the release of energy from explosive reaction. The burning rate of a high explosive at a pressure of 34.47 MPa (5000 psi) is known to be too slow to support an assumption of instantaneous reaction. In addition in this approach, the effects of particle size are not addressed. This is an old problem encountered in the intensive study of deflagration to detonation transition of solid propellants in the 1970s. Experimental results clearly indicated that the highest burning rate of propellants of high HMX concentrations at 34.47 MPa (5000 psi) is on the order of 2.79 cm/s (1.1 in./s) (Ref. 8), too slow to support an abrupt rate growth into the km/s region corresponding to a detonation. For a pulse duration of 25 μs existing in a NONEL tube, this rate corresponds to a total erosion thickness of only 0.7 μm, which is significantly smaller as compared to a typical HMX particle size, for example, 50 μm in diameter. Thus, a burning rate analysis cannot support the propagation in a NONEL tube.

The point of departure for a new approach resides in setting up a physical model of the dynamic reaction in an explosive particle, for example, HMX. The features of the conventional model are as follows:

1) Under heating by surrounding high-temperature gases at low pressure, the surface of HMX reaches 275°C, the melting temperature of the HMX. A layer of liquid HMX is formed within microseconds that insulates the interior of the HMX particle from further temperature increase beyond 275°C.

2) At 275°C, the decomposition fraction of HMX is very small (Table 1). Therefore, a slow reaction rate would result, which cannot support the fast reaction in the NONEL tube (~25 μs), as observed earlier.

Assumptions

Our proposed analysis is based on the assumptions in the following subsections.

Operating Temperature

The key concept for attaining fast HMX decomposition is the realization of temperatures much higher than 275°C exist in the liquid state of HMX. By extrapolation of data in literature,[6] the vapor pressure p_1 of liquid HMX as a function of temperature (Kelvin) is

$$\log_{10} p_1 \text{ (mm Hg)} = 9.4027 - 24.89 \times 10^3/4.576T \qquad (1)$$

where the numerical factor 24.89 in units of kcal/mole is the latent heat of vaporization of liquid HMX (Ref. 6). The numerical factor 9.4027 is calculated by matching $p_1 = p_2 = 0.30$ mm/Hg at $T = 275$°C or 548.15 K, where p_2 is the extrapolated vapor pressure of solid HMX (Ref. 6):

$$\log_{10} p_2 \text{ (mm Hg)} = 16.18 - 41.89 \times 10^3/4.576T \qquad (2)$$

where the numerical factor of 41.89 in units of kcal/mole is the latent heat of vaporization of solid HMX (Ref. 6).

Table 2 Quasi-steady-state behaviors of NONEL tube

λ, mg/m	ℓ, μm	P, MPa (psi)
5	0.85	8.67 (1257)
7	1.20	12.13 (1760)
10	1.70	17.33 (2514)
15	2.55	26.00 (3771)
20	3.40	34.66 (5028)
25	4.25	43.33 (6285)
30	5.10	52.00 (7542)

Heating Conditions

Under high pressures in a NONEL tube, combined normal heating and possible superheating[9] in melted HMX will occur; that is, in the liquid surface layer, temperature rise continues beyond 275°C, to approximately 800°C.

HMX Decomposition

The decomposition of HMX is a progressively increasing function of temperature above the melting temperature. The fractional weight loss as a function of temperature and heating time is

$$\Delta w/w_0 = 1 - w/w_0 = 1 - \exp[-A\exp(-B/T)]t \quad (3)$$

Table 1 summarizes p_1 and $\Delta w/w_0$ for a fixed heating time of 25 μs, simulating the pulse duration in a NONEL tube, and Δt, the heating time for $\Delta w/w_0 = 0.99$, for several temperatures of interest. Here, $\Delta w/w_0$ and ΔT are calculated by using numerical values of 5×10^{19} s^{-1} and 2.65×10^4 K for A and B, respectively.[6]

Critical Temperature

It can be seen that 800°C resembles the critical temperature of HMX because the vapor pressure of 28.4 bar (418 psi) is close to typical critical pressures of organic substances.[10] [Note that the critical pressures for heavy organic molecules reported range from 12 to 44 bars. The critical temperature of HMX is not a very sensitive function of choice of the critical pressure. According to Eq. (1), 16.4 and 48.7 bars of critical pressure correspond to critical temperatures of 750 and 850°C, respectively]. Temperatures above 800°C are in the supercritical regime. The extrapolated pressures corresponding to these temperatures coincide with the operating pressure in a NONEL tube (Table 2). These temperatures also coincide with the temperatures obtained in the hot spot or air bubble initiation of HMX under shock loading.[11]

Kinetic Calculation

It appears to be reasonable to extrapolate the kinetic calculation down to 1.0 μs of decomposition time because the operation of a NONEL tube is in the microseconds regime. Further extrapolation into a shorter time regimes of 0.1 μs and 4 ns may be questionable. There are indications that when the thickness of explosive is reduced to micrometers, both ignition temperature and ignition delay increase drastically in a number of explosives,[12] that is, deviating from the kinetic characteristics in the bulk (a phenomenon that may be related to the efficient disposition of heat of decomposition in a thin-layer geometry).

Analytical Model

The physical picture of decomposition of an HMX particle in a NONEL tube is nevertheless simple. Under the transient heating duration of ~25 μs, a layer of the surface will be decomposed much faster than that usually predicted by burning-rate data. However, after the reaction zone in the tube has passed down the tube and the temperature has been rapidly reduced, the inner portion of the particles is left undecomposed, especially when the NONEL tube is operated near the condition of a propagation failure (minimum decomposition).

Steady-State Estimation

The predicted results of ballistics in a NONEL tube are summarized in Table 2.

The average HMX layer thickness ℓ is calculated from the loading density λ, HMX density of 1.84 g/cm^3, and the assumption that it is uniformly coated on the tube inner wall. The significance of the results is as follows: Knowing that the actual HMX particle size used in the tube is on the order of tens of micrometers in diameter leads to the conclusion that the majority of the tube wall is not covered by HMX. The uncovered wall forms a large heat leak surface; therefore, the peak temperature in the tube is lower than the theoretically estimated value without including heat losses.

The steady-state peak pressure P is calculated from $P = e_1\lambda/v_0$, where e_1 is the specific energy of HMX (Ref. 7) of 1387 J/g and v_0 is the tube volume per meter and assuming HMX is completely decomposed. The calculated 34.66 MPa (5028 psi) for $\lambda = 20$ mg/m is higher than the 27.58 MPa (4000 psi) reported (in a very loose sense because the actual value of λ corresponding to this pressure is not known). This also could be a result of the transient expansion of the tube during propagation[1] or the heat loss to the tube wall and heat loss due to the heating of aluminum powder and incomplete decomposition of HMX.

Heat Transfer Properties

Thermal properties of HMX as a function of temperature are not all available for the range of temperature of interest, especially for the liquid state or supercritical state. Solid HMX properties[6] are thermal conductivity, $K = 9.7 \times 10^{-4}$ cal/s-cm-°C (160°C); specific heat, $C_p = 0.323$ cal/g-°C (167°C); and thermal diffusivity, $\kappa = 1.632 \times 10^{-3}$ cm^2/s.

The average diffusivity of liquid would be much smaller than the value for its solid counterpart. A conservative value of $1/3 \times 1.632 \times 10^{-3} = 5.44 \times 10^{-4}$ cm^2/s is used because a 1.5 times decrease in K and a twofold increase in C_p are common for organic substances when they are transformed from solid state into liquid state.[13] Diffusivity of fluids in the supercritical state will be at least one order in magnitude smaller than that of the same material in solid state. The results reported in the next section are not very sensitive to the diffusivity value chosen.

Critical Linear Explosive Loading Density λ_0

This is the minimum loading density below which the NONEL tube will fail to sustain the propagation. It corresponds to the energy that is necessary to offset the energy loss to the tube wall in the reaction zone for maintaining the reaction propagation. It is dependent on the tube inner diameter and the HMX particle size. For TLX, a value of 5 mg/m was commonly quoted. A quoted much lower value of 2.7 mg/m is considered unreliable because it was likely obtained from a tube of inner diameter smaller than 1.0 mm. The control and verification of such a minute amount of HMX has been very difficult as reflected by the loosely specified loading density of 20 ± 10 mg/m and because loose powder exists in the tube. Assuming the low limit of 10 mg/m is true and a factor of two of safety margin is provided in this parameter, 5 mg/m can be chosen as the critical loading density for the 1-mm-i.d. TLX. Its corresponding 8.67 MPa (1257 psi) peak pressure (Table 2) is consistent with an often-quoted TLX ignition pressure threshold.

The approximate 25-μs reaction duration is consistent with the heat loss calculation and with assumption of loading densities. It is the characteristic heat transfer time constant of the HALAR tube with 1 mm i.d. By the use of known thermal properties of HALAR, that is, $\rho = 1.68$ g/cm^3, $C_p = 0.37$ cal/g-°C, $K = 3.75 \times 10^{-4}$ cal/s-cm-°C, $\kappa = 6.03 \times 10^{-4}$ cm^2/s, and approximate heat transfer analysis, with a 2500°C temperature rise in 25 μs, approximately 6 cal/m of heat would be lost from the gas to the HALAR wall. [Note that the thermal penetration depth into the HALAR interior wall $(25\ \mu\text{s} \times \kappa)^{1/2}$ is 1.23 μm, which corresponds to 6.5 mg/m of HALAR. A temperature rise of 2500°C in the layer would provide a heat loss of ~6.0 cal/m.] This is comparable to the total heat energy (using 1.48 kcal/g of explosion energy from Ref. 7) available in a NONEL tube with 5-mg/m HMX loading density, 7.4 cal/m. This logic further substantiates the assumption that a 5-mg/m loading

density as the threshold of propagation in a 1-mm i.d. NONEL tube.

Propagation in a Bare Segment

The quantitative aspect of propagation in a bare segment in a NONEL tube, that is, without explosive impregnation, can be misleading. First, the length of the gap in which propagation could sustain depends on the loading density. Second, it is not a steady-state phenomenon. In steady state, once the reaction front has passed a location in the tube, the decomposition rate of remnant HMX particles will drastically slow down. It can only contribute to the residual temperature and pressure in the reacted part of the tube [for $\lambda = 20$ mg/m, roughly estimated values are $P \cong 3.45$–6.89 MPa (500–1000 psi), and $T \cong 400$–1000°C]. The length of the propagating reaction zone is only 25 μs $\times$ 1.9 km/s = 4.75 cm. It is estimated that the energy content of a fully reacted 20 mg/m reaction zone can sustain accumulative heat loss in four times of zone lengths before it reaches a level corresponding to a fully reacted 5-mg/m reaction zone, that is, the maximum gap length is 4 $\times$ 4.75 cm = 19 cm. This estimated result is consistent with statements made in the earlier section Information in Public Domain. The length will be reduced at low loading densities, approximately 4.75 cm for $\lambda = 5$ mg/m.

Average Temperature in the Reaction Zone

By the use of the peak pressure values calculated in Table 2 based on HMX specific energy and the handbook-listed STP specific gas volume of 927 cm^3/g for HMX (Ref. 7), a peak temperature of 3680°C is obtained. This temperature is independent of the loading density in this estimate and is higher than the approximately 3000°C of steady-state temperature in a rocket motor loaded with HMX-based propellant. Heat losses through the tube wall, resulted in a lower temperature. The boiling temperature of aluminum, 2500°C, is close to the average temperature in the reaction zone because it is believed that the tube operates in an aluminum vapor-phase reaction mode. This temperature corresponds to a gas velocity of approximately 1.45 km/s, close to the reported reaction propagation velocity in TLX.

Other Assumptions

The exact amount of aluminum used in some NONEL tubes is manufacturer's proprietary information, but it is usually small. Therefore, its effects are not analyzed. From solid propellant experience, the presence of up to 10% aluminum has a small impact on propellant burn temperature and pressure. Because the thermal diffusivity of aluminum is high (~0.85 cm^2/s), the aluminum particles in the NONEL tube will be completely melted and vaporized in 25 μs. The particle size distribution of HMX is not known with accuracy; therefore, in this first-cut analysis, uniform spherical HMX particles are assumed for simplicity of the analysis. Also, during the reaction, the particles are likely to be airborne due to the high-pressure gas flow in the tube reaction zone. Therefore, an isotropic heating of the particles is assumed.

Formulation of Analysis

With the foregoing groundwork, the following analysis is straightforward for an HMX particle. The first governing equation is derived as follows. The minimum HMX mass per unit length decomposed in the reaction zone for sustained propagation is the number of HMX particles times volume decomposed and density of HMX, that is,

$$\lambda_0 = N(4\pi/3)(a^3 - r^3)\rho$$

(5 mg/m). Because $N = \lambda/[(4\pi/3)a^3\rho]$,

$$\lambda[1 - (r/a)^3] = \lambda_0 \tag{4}$$

(5 mg/m). This equation states that, at the threshold of sustained propagation, the total mass of HMX particles decomposed in the NONEL tube reaction zone shall equal 5 mg/m, the critical loading density. This establishes that there is a relationship between λ and r/a as shown in Fig. 2.

The analytical solution of heating a sphere at temperature T_0 by a constant surrounding temperature $T_{surface}$ can be found in the literature.[14] The normalized temperature $(T - T_0)/(T_{surface} - T_0)$ as a function of normalized radial position $x = r/a$ is described in the following equation obtained by solving the heat transfer differential equation in spherical coordinates and boundary conditions:

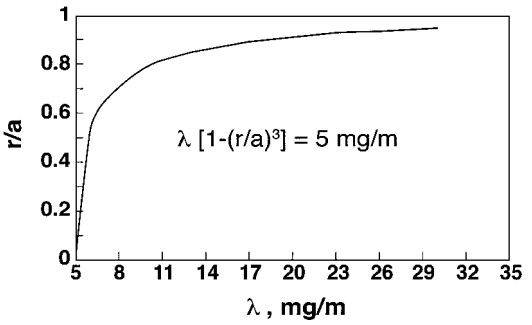

Fig. 2 Normalized decomposition radius vs linear loading density.

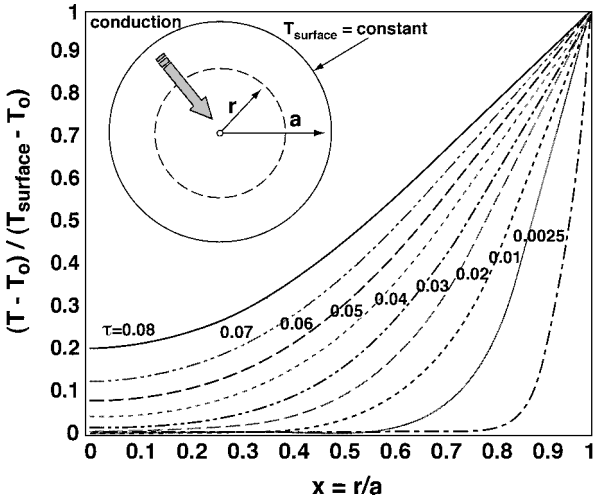

Fig. 3 Heat transfer in a spherical HMX particle under a constant surface temperature.

$$\frac{T - T_0}{T_{surface} - T_0} = \frac{1}{x}\sum_{n=1}^{\infty}\left[\operatorname{erfc}\left(\frac{(2n+1) - x}{2\sqrt{\kappa t/a^2}}\right) - \operatorname{erfc}\left(\frac{(2n+1) + x}{2\sqrt{\kappa t/a^2}}\right)\right], \qquad x = r/a \tag{5}$$

A plot of this equation is shown in Fig. 3 using normalized time τ as a parameter. The steps for calculating of the regression of an HMX particle due to surface heating resulted decomposition are as follows:

1) For the high ambient temperature, a liquid layer will form on the surface.

2) The propogation rate of this liquification front is not as high as indicated by the leading edge of the heat penetration in Fig. 3 because the HMX latent heat of liquification of 57.4 cal/g is comparable to the energy for heating of HMX from the ambient of 20–275°C, 76.8 cal/g.

3) The decomposition of liquid HMX at 275°C in 25 μs is negligible for the interpretation of ballistics in a NONEL tube (Table 1).

Under the operating pressure in a NONEL tube, 6.90–27.58 MPa (1000–4000 psi), the highest attainable $T_{surface}$ is about 1000°C $\pm$ 50°C (Table 1). Therefore, evaporation of HMX will occur. The evaporated HMX does not participate in the ballistics of NONEL tube directly because the milliseconds regime[8] gaseous reaction time is much longer than 25 μs. The evaporation rate is small due to the low thermal conductivity and low density of the supercritical HMX that buffers the high-temperature gas from the HMX particle. Therefore, it is overriden by the liquid decomposition rate

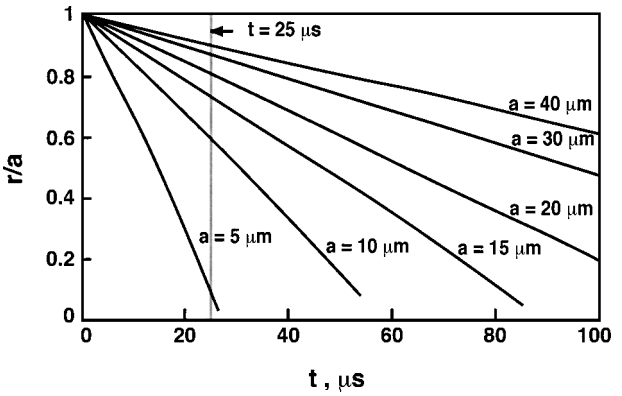

Fig. 4 Regression of HMX in 1.0-θs time increments for different initial particulate radius.

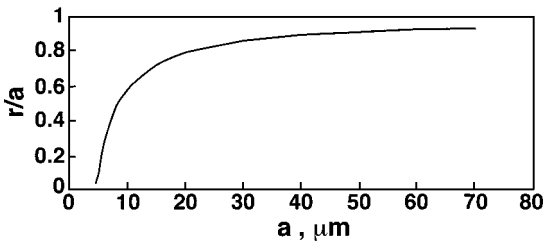

Fig. 5 Normalized decomposition radius for $t = 25\,\theta$s as a function of a.

described in the next paragraph. It is suspected that this low evaporation rate, which is often described for the diffusion zone or mixing zone of vapors of fuel and oxidizer in the analysis of solid propellant combustion, might have contributed to the low regression rate reported in Ref. 8. In our scenario, a minimum temperature on the order of 1200°C is required in the gaseous phase in the NONEL tube reaction zone to sustain the efficient heat transfer from the gases to the HMX surface.

The most significant HMX decomposition occurs in the liquid layer with temperature between 609.7 and ~800°C. The exact decomposition time is not known for certain in this temperature range, that is, the HMX is in a quasi-gaseous state. However, as stated earlier, it is reasonable to expect that in 1.0 μs time it will be completely decomposed. Therefore, the regression is calculated in consecutive 1.0-μs increments, using $T = 609.7$°C as the criterion for decomposition radius r and assuming the liquid density is the same as the solid density: $\kappa = 5.44 \times 10^{-4}$ cm^2/s, $T_{\text{surface}} = 800$°C, and $T_0 = 275$°C (the melting temperature is essentially constant for the pressures range in the tube).

Figure 4 shows the results for several particulate radii of interest, presented as r/a vs t with a as the control parameter. The normalized decomposition radius r/a at $t = 25\,\mu$s is plotted as a function of a in Fig. 5. Regression rates $\dot{r}_0$ of 0.160–0.172 μm/μs are obtained (a decreasing function of a). Because of the HMX decomposition in the gaseous phase is not considered as important in supporting the reaction propagation in the NONEL tube, $\dot{r}_0$ is not a sensitive function of pressure in the tube as in the case of combustion of solid propellants. However $\dot{r}_0$ is implicitly dependent on the pressure because the pressure controls the heating of HMX via vapor pressure–temperature relationship [Eq. (1) and Table 1].

By the combining of the results from Figs. 2 and 5, a relationship between the loading density λ and the maximum allowable average HMX particle diameter or critical diameter, D_c or $2a_c$, can be obtained as shown in Fig. 6. Numerical critical average diameters of interest are given in Table 3. A further detailed discussion of the physical meaning of D_c based on the energy balance equation is included in the Appendix.

These results indicate that D_c is a sensitive function of λ. Because a large tolerance exists in the control of λ in NONEL tube manufacturing, a good strategy is to use fine particle diameter below 20 μm to enhance propagation reliability in the low λ regime of 5–10 mg/m. However, from a practical perspective, the finest ready-to-use HMX

Table 3 Critical average HMX diameters for typical HMX loading densities of interest

λ, mg/m	D_c, μm
5	8.8
7	25.0
10	40.8
15	65.6
20	89.8
25	113.7
30	137.5

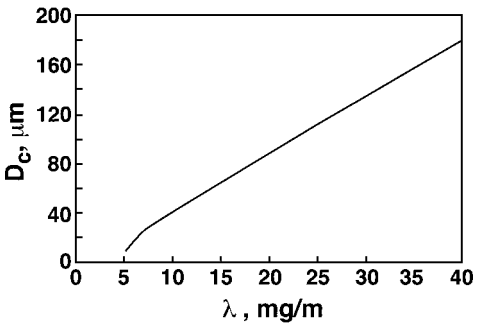

Fig. 6 Critical average HMX diameter vs linear loading density.

per MIL-H-45444 (Ref. 15) class 5 does not meet the criterion of this approach. The requirement for class 5 is that a minimum of 98% of HMX shall pass standard sieve number 325; that is, particle diameter as large as 57 μm is allowed. It is apparent that using finer sieves, or milling class 5 HMX, or a combination of both will be needed for finer HMX particle size control suitable for NONEL tube fabrication. As an aside, in high-energy propellant manufacturing, HMX particle size on the order of 5 μm is routinely controlled.

Another benefit of using finer HMX is that it may improve the adhesion of particles on the tube's inner wall. The lower profile of the particles can minimize the impact of a flow-induced powder migration failure mode and offers additional resistance to flow when the particles are trapped in the voids existing on the inner tube wall surface due to roughness. Fine particles offer better results because good adhesion can also improve powder loading control and reduce the powder distribution variation. Furthermore, in this regard, one explosive powder mechanical stabilization technique is worth consideration. Reprecipitated fine needle-shaped PETN crystals (micrometers in diameter and tens of micrometers in length) are commonly used in an exploding bridgewire detonator for maintaining a stable low PETN density (1.0 g/cm^3). In addition to the enhancing mechanical stability, the large surface area provided by small diameter particles should also enhance the reaction efficiency in a NONEL tube.

End-Tip Transfer Failure Analysis

HE end-tip to LE end-tip transfer failure is the second important NONEL tube assembly failure mode investigated. Other credible failure modes, for example, moisture contamination, cut tube, and severely pinched tube, are not addressed here.

The detonating end-tip design is widely in use in conjunction with confined detonating cords (CDCs). Although a small core load on the order of 0.53 g/m (2.5 grains/ft) of PETN, RDX, and HNS can be reliably propagated, it does not have sufficient output energy for detonation transfer between the cords or between the cords and other explosive trains. An end tip containing approximately 64.7–129.0 mg (1–2 grains) of high explosive (same as that used in the CDC) in an end cup is used. The transfer function between two detonating explosive-based end tips is well understood.[16] The shock and fragments generated by the donor end tip set off the acceptor end tip. The phenomenon is quantified by measurement of the velocity of the flyer plate formed by the closure disk and side wall of the donor end tip.

The HE end tip for NONEL ETS is basically similar to the detonating end tip in CDCs, except a lead azide increment is used in the explosive train as an intermediate deflagration to detonation charge between the NONEL tube and the detonating output charge. Propagation transfer from a detonating source to NONEL tube is fairly easy. In the Primadet applications, multiple NONEL tubes, for example, six tubes, can be initiated simultaneously by one detonating cord or a detonating end tip in a side-to-side configuration. No intermediate pyrotechnic ignition charge is necessary. The adoption of an LE end tip, including an ignition pyrotechnic charge in front of the TLX (ignition strand), originates from the F-16 aircraft application in which TLX lines are used in multiple interconnected configurations through a manifold or union.[4] The LE end tip was designed mainly for the TLX output enhancement for LE-to-LE end-tip transfer in the manifold or union. The use of an LE end tip as an acceptor for an HE end tip was presumably the result of standardization of hardware rather than a mandated need. The introduction of an ignition pyrotechnic charge adds an additional element that must be made reliable for a NONEL ETS. The transfer from HE end tip to LE end tip in a NONEL ETS is unique; criteria for its functional reliability are not well reported. The fundamental question concerns which mechanism is more efficient in this transfer mode; either the flyer plate or the hot gas, although both are accompanying an HE end-tip output. Our approach to the question is to use the CTH hydrodynamic code formulated by the Sandia National Laboratories[17] to analyze the typical HE-to-LE end-tip transfer configuration.

Because the equation of state (EOS) and constitutive equation (CE) used in CTH are not available for lead azide, silicon seal, and deflagration pyrotechnics in the CTH database, EOS and CE of other similar material were used: EOS for PETN was used for lead azide, and the EOS for nylon and CE for polyethersulfon were used for the rubber seal and the HALAR plastic. Aluminum was used to simulate pyrotechnics in the LE acceptor end tip because it has well-known properties. Our objective was to use the analysis as a gauge for the temperature and pressure responses at the input to the pyrotechnic interface only. Predicting of fracture in CTH is being intensively improved. Success is on a case-by-case basis. To simulate flyer plate and blasting plume formation, various artificially prefractured structures, for example, holes, isolated closure disk, and gaps, were included in the input. This approach turned out to work well for our intended purpose.

Figure 7 shows the model simulating an HE end tip coupled to an LE end tip in a cylindrical coupler configuration. The dimensions and materials are close to those used in typical hardware.[4,5] Densities of 1.77 g/cm^3 for PETN and 1.69 g/cm^3 for HNS-I were used for the simulation. A nominal gap of 0.127 cm (0.050 in.) between the HE and LE end tips was set. An additional 0.127 cm (0.050 in.) recess, which exists in the face of the LE end tip, was also included. This recess provides handling protection for the pyrotechnic charge. The $ZrKClO_4$ pyrotechnic in the LE was designated because the real composition of the ignition strand is proprietary. The backside of the acceptor end tip was closed by nylon plastic rather than representing a NONEL tube in the real hardware. The NONEL tube was not simulated because CTH cannot model the propagation mechanism, due to the small amount of HMX. Therefore, no meaningful result could be obtained in this explosive train interface. Two rows of tracer points were incorporated near the critical region between the two end tips and in the upstream part of the LE end tip for monitoring time profiles of pressure and temperature at these locations.

The results of six cases, including the most probable HE end-tip fragmentation modes, are presented in Table 4 and Figs. 8a–8f. In

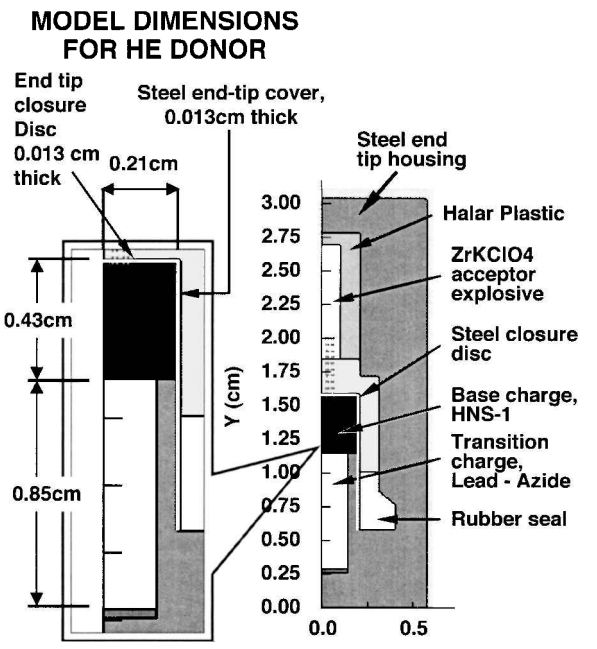

Fig. 7 Model of detonating (HE) end tip coupled with a nondetonating (LE) end tip.

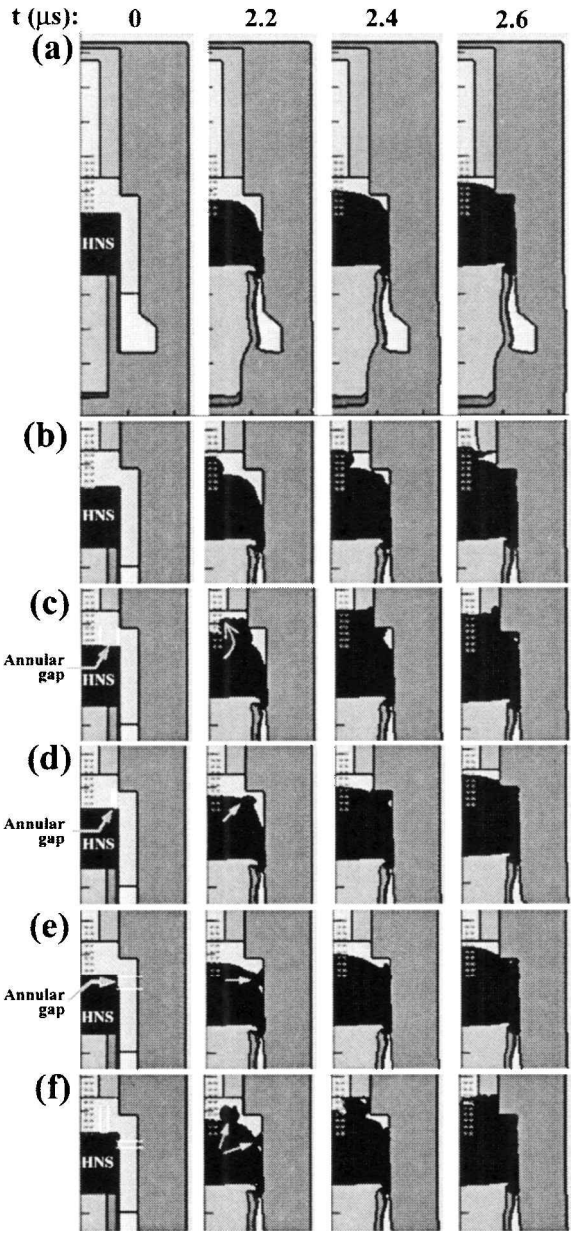

Fig. 8 CTH simulation results, material–time history: a) run 1 baseline configuration, b) run 2 central hole (radius = 0.05 cm) in closure disk, c) run 3 large annular gap (width = 0.078 cm) in the rim edge of the closure disk, d) run 4 small annular gap (width = 0.01 cm) in the rim edge of the closure disk, e) run 5 annular gap (width = 0.088 cm) in the lateral wall of the end cap at the joint to the closure disk, and f) run 6 annular gaps (widths = 0.04 cm) in both closure disk rim edge and lateral end cap wall.

Table 4 Results summary for CTH simulation of detonating (HE) end-tip to nondetonating (LE) end-tip transfer

Run number	Configuration	First impact	t, μs	V_i, km/s	P_i, GPa	T_i, K
1	Fully covered	Disk	2.7	1.4	22.5	2000, 2800
2	Central hole on closure disk	Gas	2.25	2	16.0	5000, 2000
3	Big top annular gap	Gas	2.7	1.05	23.0	8000
4	Small top annular gap	Disk	2.65, 4.0	1.4, 1.6	22.0, 2.0	2000, 3000
5	RHS annular gap	Disk	2.65, 4.0	1.4, 1.3	26.0, 2.5	2000, 3300
6	Top and RHS annular gaps	Gas	2.4	0.75	12.0	4500

each case, the PETN in the donor HE end tip is artificially detonated at the rear end at time zero and reached steady-state propagation quickly to initiate the HNS output charge. The approximate 1.7 length-to-diameter ratio of the HNS column allows a steady-state detonation to be achieved in the HNS halfway through the column. Material profiles as a function of time are presented in these Figs. 8. Figure 8a is the baseline case in which no artificial prefracture in the end tip was introduced. As expected, the closure cup of the HE end tip exhibited nearly uniform balloon expansion. When prefractures are included, gas plumes are observed, due to their higher velocities. The inertial confinement effect of the 0.0127-cm- (0.005-in.-) thick steel end cup dramatically affected the dynamic behavior of the gases.

The following provides a brief description of the contents of Table 4: The configuration column describes the prefracture condition. The numerical conditions are included in the corresponding titles of Figs. 8a–8f. (RHS refers to the right-hand side in Fig. 8 but actually is in cylindrical symmetry.) The first impact column defines either hot gas or the closure disk flyer plate. Time of impact of either gas or disk on the LE explosive (initial impact and second impact) is under the t heading. Velocity at impact (initial impact and the second impact) is listed under V_i. Pressure at impact (initial value and the second peak) is listed under P_i. Temperature at impact (initial value and the second peak) is listed under T_i.

The following observations can be made. In runs 2, 3, and 6, the gas impacts the LE pyrotechnic interface first, which generates an impact temperature much higher than in those cases in which the closure disk flyer plate impacts first. Therefore, the gas would be more effective in initiating the pyrotechnic in an LE end tip. Because of the short duration of the impact-generated heat pulse (~ 1 μs) and because the actual temperature induced in a pyrotechnic was lower than our case with aluminum, failure to initiate could result if the disk impacted first. This would be especially true at low test temperatures, for example, -53.9°C. Furthermore, the disk has the effect of isolating the LE explosive from direct contact with the plume, thereby reducing initiation effectiveness. These assessments support a potential HE-to-LE end-tip failure mode described in Ref. 3 but with a different interpretation. Failure can occur that is not necessarily caused by HE end-tip generated fragments damage to the LE end tip as stated in Ref. 3.

A variety of concepts can be used to achieve transfer reliability, including the use of adapters described in Ref. 3 for filtering out the closure disk. Simpler techniques to facilitate the donor closure disk fragmentation include using an etched asterisk or cross pattern on the disk for petaling and increasing the gap width between end tips because this allows more time for the gas plume to bypass the closure disk fragments and arrive at the LE end tip first.

As expected, in all three cases in which the disk impacts the LE explosive interface first, higher impact pressures were generated. The pressures induced by the gases in the cases where gaseous plume impacted first were lower, but still may have been effective in initiating an HE end tip, that is, successful HE-to-HE end-tip transfer. Run 3 produced both high pressure and high temperature at the LE explosive interface. This was different from the fragmentation scenario described in Ref. 16, in which initiation by fragments was across very large gaps. The fragments in that case quickly moved out of the gas plume in the explosive transfer across gaps because the gas plume tends to cool down rapidly in large adiabatic expansion.

Conclusions

As in all well-designed explosive devices/systems, the functional reliability of the NONEL tube ETS can be achieved through proper control of key parameters in design and manufacturing.

The key parameters analyzed in this study were tube explosive loading density and particle size in the NONEL tube and the ignition of LE explosive end tip by HE end tips. The current explosive loading density tolerance of 20 ± 10 mg/m, that is, $\pm 50\%$, for explosive loading density is inconsistent with a high reliability. Tolerances smaller than $\pm 25\%$ should be the goal for controlling this critical parameter.

A critical maximum average explosive particle diameter exists in a NONEL tube that is an increasing function of the explosive loading density. Marginal loading density, in conjunction with the large variability in loading density and coarse particle sizes that exist in current manufacturing, can cause propagation failures in NONEL tubes. For the usual explosive loading density of 10–30 mg/m, using fine particle size, for example, less than 20 μm in diameter for HMX, can increase the propagation reliability. A standard test should be included in the tube acceptance test to verify the powder adhesion.

For HE-to-LE end-tip ignition, the hot gas produced by the donor end tip is more effective than the closure disk flyer plate mechanism. A variety of concepts can be used to enhance transfer reliability.

The foregoing discussions should be helpful for understanding the operation in the NONEL tube. The suggested fine-particle approach is practically implementable and test verifiable. Our understanding is that detailed analyses, including particle size distributions, are not being performed at this time.

Appendix: Energy Balance in Reaction Zone

The following formulation is based on the quasi-steady-state energy balance in the NONEL tube reaction zone. It is an approximation with emphasis on the heat energy, which is mainly temperature dependent. The energy due to pressure is not explicit. It is envisioned that the afterburn of aluminum behind the reaction zone may support a slower pressure decay in milliseconds, causing a very small change to occur during the reaction in the reaction zone. Thus,

$$\frac{\mathrm{d}E}{\mathrm{d}t} = \left(\frac{\mathrm{d}E}{\mathrm{d}t}\right)_1 + \left(\frac{E}{\mathrm{d}t}\right)_2 \tag{A1}$$

where

$$\left(\frac{\mathrm{d}E}{\mathrm{d}t}\right)_1 = -\frac{E}{\tau_1} \tag{A2}$$

$$\left(\frac{\mathrm{d}E}{\mathrm{d}t}\right)_2 = 4\pi r^2 \dot{r}_0 \rho N e_0$$

$$= 3\lambda \dot{r}_0 (a - \dot{r}_0 t)^2 \frac{e_0}{a^3} \quad \text{for} \quad a - \dot{r}_0 t > 0 \tag{A3}$$

$$= 0 \quad \text{for} \quad a - \dot{r}_0 t \leq 0 \tag{A4}$$

These equations can be solved in closed form under the initial condition $E = 0, t = 0$. For the benefits of correlation with the earlier discussions, a typical solution is presented in Fig. A1 for $\lambda = 10$ mg/m, $\tau_1 = 25$ μs, $e_0 = 1.48$ kcal/g, $\dot{r}_0 = 0.164$ μm/μs, and HMX particle

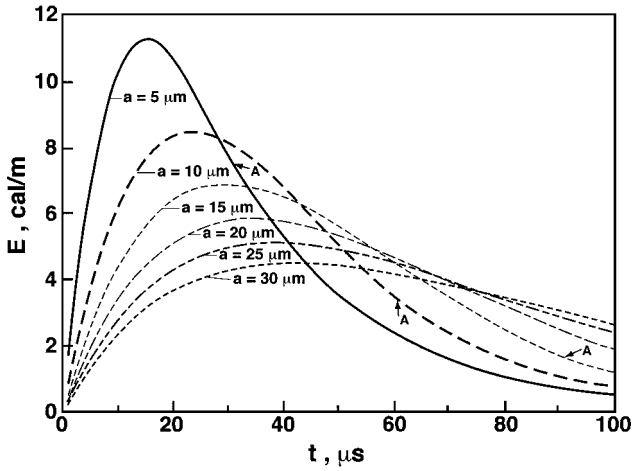

Fig. A1 Energy per unit length in the reaction zone as a function of time for $\lambda = 10$ mg/m.

radius a as a parameter. As expected, E exhibits a peak value indicating that, for the range of a used in the caluclation, the total surface area of HMX has been reduced to a level below that for effective off setting the heat loss to the tube wall. Points marked with A correspond to $(a - \dot{r}_0 t) = 0$.

The peak values of E are considerably smaller than the value $\lambda e_0 = 14.8$ cal/m, which corresponds to a theoretical temperature of ~3300°C in the reaction zone. The peak value of 11.2 cal/m for $a = 5$ μm corresponds to ~2500°C as assessed earlier. The critical average radius for $\lambda = 10$ mg/m, $a_c = 20.4$ μm (Table 3) corresponds to a peak $E \cong 5.5$ cal/m or $T \cong 1226$°C. For NONEL tube propagation, 1226°C can be viewed as a critic temperature. It is seen that the results for $a = 25$ and 30 μm were invalid because they correspond to temperatures much lower than this critical temperature for propagation. Under this circumstance, the regression rate would be drastically reduced from that indicated in Fig. 4. Failure to propagate results.

Because E is linearly dependent on λ, Fig. A1 can be used to assess cases for different λ by scaling. It is seen that, for $\lambda = 5$ mg/m, the peak value of E for $a = 5$ μm is $1/2 \times 11.2$ cal/m $= 5.6$ cal/m, very close to the nonpropagation energy density (energy per unit length). Referring to the 5.5 cal/m, a minimum energy density criterion, all curves in Fig. A1 have a full-width half-maximum duration of approximately 25 μs, an indication that the duration of reaction is not a sensitive function of λ and a.

Acknowledgments

The many contributions of information, discussions, and support for this work are appreciated: S. Perkins and J. Fritz of the Ensign-Bickford Co.; B. Paul, S. McDonald, and C. Russell of OEA Aerospace, Inc.; P. A. Persson of New Mexico Technical University; E. S. Hertel Jr. of Sandia National Laboratories; T. Blachowski and P. Renn of the U.S. Naval Surface Warfare Center; J. Gormley of Lockheed Martin; T. Moore of the Chemical Propulsion Information Agency, Johns Hopkins University; and J. Wee, D. P. Harry, B. G. Morton, J. N. Mason, S. M. Vierra, and E. F. Zabrensky of TRW.

References

[1]Persson, P. A., "Fuze," U.S. Patent 3,590,739, 6 July 1971.

[2]Persson, P. A., Holmberg, R., and Lee, J., *Rock Blasting and Explosive Engineering,* CRC Press, Boca Raton, FL, 1996, pp. 145–167.

[3]"Saga of Delta 3's Problems with Thin-Layered Explosives," *Florida Today, Space Online*, URL: www.floridatoday.com/space/ [cited 26 Aug. 1998].

[4]Early, W. E., Jr., "The Use of TLX Energy Transfer Lines on the F-16 Aircraft," Pyrotechnics and Explosives Application Section of the American Defense Preparedness Association (now National Defense Industrial Association); Defense Technical Information Center, AD-A143-157, Ft. Belvoir, VA, Sept. 1983.

[5]Ratts, J. F., "Qualified Polymer Sheathed Explosive Cord in Air Crew Escape/Egress Systems," AIAA Paper 95-2544, July 1995.

[6]Gibbs, T. R., and Popolato, A., *LASL Explosive Property Data*, Univ. of California Press, Berkeley, CA, 1980, pp. 46, 47.

[7]Meyer, R., *Explosives*, 3rd ed., VCH Verlagsgesellschaft, Weinheim, Germany, 1989, pp. 233, 234.

[8]Boggs, T. L., Price, C. F., Zurn, D. E., and Derr, R. L., "Role of Gas Phase Reaction in Deflagration-To-Detonation Transition," *Proceedings of Seventh Symposium (International) on DETONATION*, U.S. Naval Surface Weapons Center, MP 82-334, Dahlgren, VA, 1981, pp. 216–224.

[9]Skripov, V. P., *Metastable Liquids*, Wiley, New York, 1974.

[10]Vargaftik, N. B., *Handbook of Physical Properties of Liquids and Gases—Pure Substances and Mixtures*, 2nd ed., Hemisphere, Washington, DC, 1975.

[11]Mader, C. L., *Numerical Modeling of Explosives and Propellants,* 2nd ed., CRC Press, New York, 1998, pp. 164–166.

[12]Bowden, F. P., and Yoffe, A. D., *Fast Reaction in Solids*, Academic, New York, 1958, pp. 28–32.

[13]Perry, R. H., and Chilton, C. H., *Chemical Engineers' Handbook*, 5th ed., McGraw–Hill, New York, 1975, Tables 3-177 and 3-178, pp. 3-126–3-133.

[14]Carslaw, H. S., and Jaeger, J. C., *Conduction of Heat in Solids*, 2nd ed., Clarendon, Oxford, 1959, pp. 233, 234.

[15]"Military Specification, HMX," Armanent Research and Development Engineering Center, U.S. Army, MIL-H-45444B, Picatinny Arsenal, NJ, Feb. 1974.

[16]Schimmel, M. L., "Quantitative Understanding of Explosive Stimulus Transfer," NASA CR-2341, Dec. 1973.

[17]Hertel, E. S., Bell, R. L., Elrick, M. G., Farsworth, A. V., Kerley, G. I., McGlaun, J. M., Petney, S. V., Silling, S. A., Taylor, P. A., and Yarrington, L., "CTH, A Software Family for Multi-Dimensional Shock Physics Analysis," *Proceedings of the 19th International Symposium on Shock Waves*, edited by R. Burn and L. D. Dumitrescu, Vol. 1, Springer-Verlag, Berlin, 1995, pp. 377–382.

M. Sichel
Associate Editor